Integration of dynamic parameters in the analysis of ^{18}F-FDopa PET imaging improves the prediction of molecular features of gliomas

Merwan Ginet, Timothée Zaragori, Pierre-Yves Marie, Véronique Roch, Guillaume Gauchotte, Fabien Rech, Marie Blonski, Zohra Lamiral, et al.

European Journal of Nuclear Medicine and Molecular Imaging

ISSN 1619-7070

Eur J Nucl Med Mol Imaging
DOI 10.1007/s00259-019-04509-y

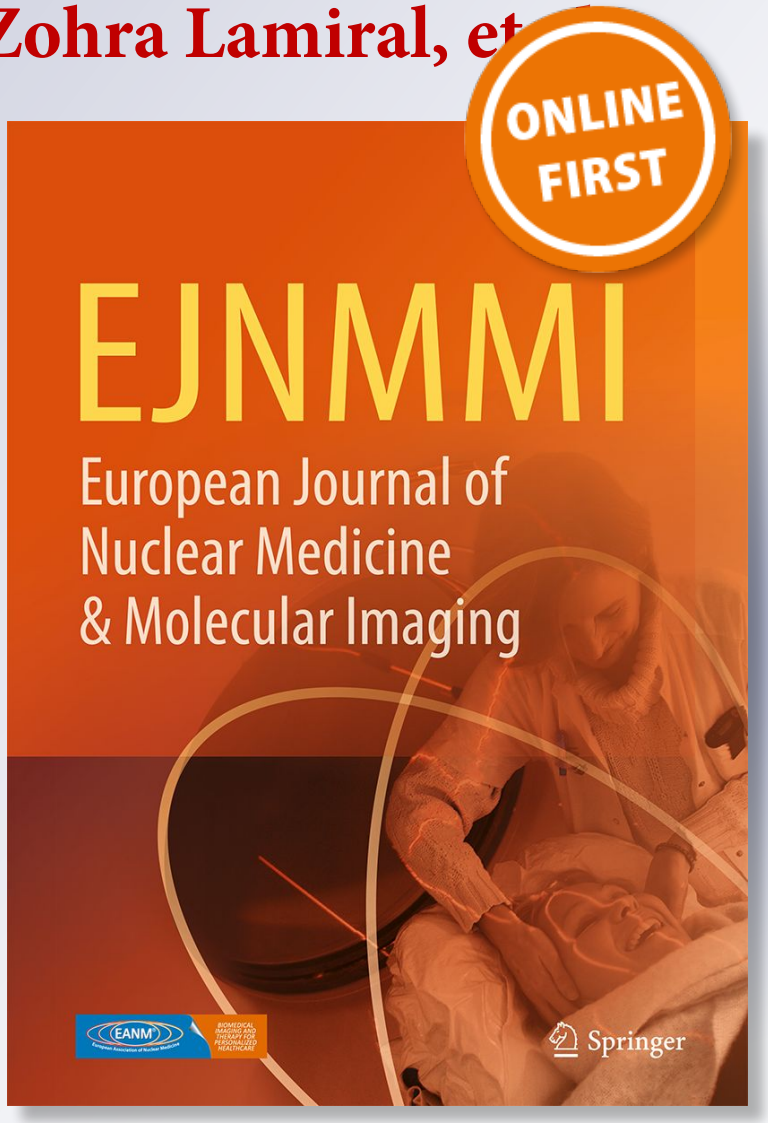

Springer

European Journal of Nuclear Medicine and Molecular Imaging
https://doi.org/10.1007/s00259-019-04509-y

ORIGINAL ARTICLE

Integration of dynamic parameters in the analysis of ^{18}F-FDopa PET imaging improves the prediction of molecular features of gliomas

Merwan Ginet[1] · Timothée Zaragori[1,2] · Pierre-Yves Marie[1,3] · Véronique Roch[1] · Guillaume Gauchotte[4,5] · Fabien Rech[6,7] · Marie Blonski[6,7] · Zohra Lamiral[3] · Luc Taillandier[7,8] · Laëtitia Imbert[1,2] · Antoine Verger[1,2]

Received: 24 April 2019 / Accepted: 23 August 2019

Abstract

Purpose ^{18}F-FDopa PET imaging of gliomas is routinely interpreted with standardized uptake value (SUV)-derived indices. This study aimed to determine the added value of dynamic ^{18}F-FDopa PET parameters for predicting the molecular features of newly diagnosed gliomas.

Methods We retrospectively included 58 patients having undergone an ^{18}F-FDopa PET for establishing the initial diagnosis of gliomas, whose molecular features were additionally characterized according to the WHO 2016 classification. Dynamic parameters, involving time-to-peak (TTP) values and curve slopes, were tested for the prediction of glioma types in addition to current static parameters, i.e., tumor-to-normal brain or tumor-to-striatum SUV ratios and metabolic tumor volume (MTV).

Results There were 21 IDH mutant without 1p/19q co-deletion (IDH+/1p19q−) gliomas, 16 IDH mutants with 1p/19q co-deletion (IDH+/1p19q+) gliomas, and 21 IDH wildtype (IDH−) gliomas. Dynamic parameters enabled differentiating the gliomas according to these molecular features, whereas static parameters did not. In particular, a longer TTP was the single best independent predictor for identifying (1) IDH mutation status (area under the curve (AUC) of 0.789, global accuracy of 74% for the criterion of a TTP ≥ 5.4 min) and (2) 1p/19q co-deletion status (AUC of 0.679, global accuracy of 69% for the criterion of a TTP ≥ 6.9 min). Moreover, the TTP from IDH− gliomas was significantly shorter than those from both IDH+/1p19q− and IDH+/1p19q+ ($p \leq 0.007$).

Conclusion Prediction of the molecular features of newly diagnosed gliomas with ^{18}F-FDopa PET and especially of the presence or not of an IDH mutation, may be obtained with dynamic but not with current static uptake parameters.

Keywords ^{18}F-FDopa PET · Dynamic analysis · Glioma · Diagnosis · WHO 2016 classification · IDH mutation

Merwan Ginet and Timothée Zaragori contributed equally to this work.

This article is part of the Topical Collection on Oncology – Brain

Electronic supplementary material The online version of this article (https://doi.org/10.1007/s00259-019-04509-y) contains supplementary material, which is available to authorized users.

✉ Antoine Verger
a.verger@chru-nancy.fr

[1] CHRU-Nancy, Department of Nuclear Medicine & Nancyclotep Imaging platform, Université de Lorraine, F-54000 Nancy, France

[2] IADI, INSERM, UMR 1254, Université de Lorraine, F-54000 Nancy, France

[3] Université de Lorraine, INSERM U1116, F-54000 Nancy, France

[4] CHRU-Nancy, Department of Pathology, Université de Lorraine, F-54000 Nancy, France

[5] INSERM U1256, Université de Lorraine, F-54000 Nancy, France

[6] Department of Neurosurgery, CHU-Nancy, F-54000 Nancy, France

[7] Centre de Recherche en Automatique de Nancy CRAN, CNRS UMR 7039, Université de Lorraine, F-54000 Nancy, France

[8] CHRU-Nancy, Department of Neuro-oncology, Université de Lorraine, F-54000 Nancy, France

Published online: 16 September 2019

Introduction

The radiolabeled amino acid positron emission tomography (PET) imaging of gliomas is increasingly used for diagnostic and prognostic purposes, both for treatment planning and for tumor monitoring (whether under oncological treatment or without any treatment), including the specific diagnosis of glioma recurrence [1–5]. The Response Assessment in Neuro-Oncology (RANO) working group has recommended its use in these settings as a complement to standard magnetic resonance imaging (MRI) [6].

Until now, studies with 6-[^{18}F]fluoro-L-DOPA (^{18}F-FDopa), an amino acid PET radiotracer approved and currently used in Europe for assessing recurrent brain tumors [7–10], have been mainly performed using standard uptake value (SUV)-derived indices such as tumor-to-brain or tumor-to-striatum ratios [7–9, 11, 12]. Albeit less used in routine practice, the metabolic tumor volume (MTV) has also been shown to be informative in this setting [13]. However, this standard analysis does not take into account the dynamic information previously shown to markedly improve the grading of gliomas, although this improvement was established for PET recorded with O-(2-[^{18}F]fluoroethyl)-L-tyrosine (^{18}F-FET), another amino acid radiotracer extensively used in glioma imaging [14, 15]. In these dynamic ^{18}F-FET studies, low-grade gliomas typically show a continuous increasing slope with a late time-to-peak, as opposed to an early time-to-peak, followed by a steeper slope in high-grade gliomas [14, 15]. Dynamic data of ^{18}F-FDopa were previously analyzed in only a few pilot studies [16–18], without considering the molecular characteristics involved in the World Health Organization (WHO) 2016 classification of gliomas, and only by modeling tracer kinetics with multi-compartmental models [19]. For routine ^{18}F-FET PET imaging, it has however been shown that a much more simple analysis of time-activity curves can provide key information for tumor characterization [14, 15].

In addition, the WHO classification of gliomas has recently been upgraded with the introduction of molecular parameters including IDH (isocitrate dehydrogenase enzyme isoform) mutation and 1p/19q co-deletion, leading to improve the link with patient prognosis [19]. In particular, the presence of an IDH mutation at initial diagnosis is strongly associated with an enhanced prognosis [19]. The correspondence with this new glioma classification has since been analyzed for PET performed with amino acids other than ^{18}F-FDopa [20–23] or more recently with ^{18}F-FDopa PET using only static parameters and with inconclusive results [24]. Notwithstanding the latter, the potential effect of IDH mutation on ^{18}F-FDopa uptake has been suggested in diffuse gliomas [25, 26].

In light with the above, this study aimed to determine the added value of dynamic ^{18}F-FDopa PET parameters for predicting the molecular features of newly diagnosed gliomas according to the WHO 2016 classification.

Material and methods

Patients

Consecutive patients in whom ^{18}F-FDopa PET imaging was performed for a newly diagnosed glioma were retrospectively selected, and only those for whom the dynamic PET parameters and the features of IDH mutation and 1p/19q co-deletion status were available according to the WHO 2016 classification [19], were included for the final analysis. In addition, the time window between PET imaging and neuropathological confirmation was 56.0 (9.3; 109.0) days [8]. A flowchart describing patient selection is provided in Supplemental Fig. 1. The local ethics committee (Comité d'Ethique du CHRU de Nancy) approved the retrospective data evaluation on June 7, 2018, and the CNIL (National Commission on Information Technology and Liberties) number authorization was delivered on June 25, 2018 (R2018-11). This research complied with the principles of the Declaration of Helsinki. Informed consent was obtained from all individuals included in the study.

PET recording and reconstruction

^{18}F-FDopa PET-computed tomography (CT) scans were obtained on a Biograph hybrid system involving a six-detector CT for attenuation correction (Biograph 6 True Point, SIEMENS, Erlangen, Germany). Patients were instructed to fast for at least 4 h and certain patients received Carbidopa administration 1 h prior to their exam, the latter having been shown to increase striatal dopaminergic activity [27], as well as brain tumor uptake [16]. The CT scan was first recorded and immediately followed by a 30-min 3D list-mode PET recording initiated during the bolus injection of 3 MBq of ^{18}F-FDopa per kilogram of body weight. The static PET images were reconstructed with the list-mode data acquired from 10 to 30-min post-injection [9, 28] while the dynamic PET images involved 6 consecutive frames of 20 s each followed by 28 frames of 1 min each [18].

All images were reconstructed with an OSEM 2D algorithm (2 iterations, 21 subsets, 4-mm Gaussian post-reconstruction filter), corrected for attenuation, scatter, and radioactive decay, and displayed in a 256 × 256 matrix with 2.7 × 2.7 × 3.0 mm^3 voxels.

Analyses of PET images

Different regions of interest (ROIs) were placed on the static PET images using a dedicated software (Oasis, Nicesoft, Paris, France). These consisted of two spherical ROIs of 2-cm diameter each, the first of which was centered on the tumor area of maximum uptake [17] for determining maximal and mean standardized uptake values (SUV_{max} and SUV_{mean}, respectively) of the tumor, and the second on the contralateral basal ganglia for the computing of tumor-to-striatum (TSR)

ratios. An elliptic ROI (2 × 4 cm) was additionally positioned on the semi-oval center of the unaffected contralateral hemisphere, including white and gray matter [9], for the computing of tumor-to-normal brain (TBR) ratios. TSR and TBR were computed as SUV_{mean} or SUV_{max} of the tumor divided by the SUV_{mean} of the striatum (TSR_{mean} and TSR_{max}) or of normal brain (TBR_{mean} and TBR_{max}).

The tumor could not be detected on ^{18}F-FDopa PET images ($TBR_{max} < 1.6$) in 10 cases where the tumor ROIs were placed at the site of the MRI abnormalities with a fused display of PET and Fluid Attenuation Inversion Recovery (FLAIR) MRI images [9].

As previously described, the metabolic tumor volume (MTV) was obtained through a 3D auto-contouring process with a threshold corresponding to the SUV_{mean} of the contralateral striatum [13].

In addition, given that TBR values are likely to be much less influenced by Carbidopa premedication than SUV, time-activity curves, representing the evolution of the TBR_{mean} as a function of time (TAC_{ratio}), were extracted with the PLANET® Dose software (DOSIsoft, Cachan, France) and with the ROIs previously placed on the static images (see above). Each dynamic frame was previously registered on the CT images, to take into account potential patient movements during acquisitions [29]. Two dynamic parameters were determined from fitted curves to overcome noise effects, using a method already validated for ^{18}F-FET in the same setting [30], namely (i) time-to-peak (TTP), corresponding to the delay between the beginning of the dynamic acquisition (time of tracer injection) and the time-point of the maximal TBR_{mean} value and (ii) the slope from the 10th minute of the TBR_{mean}-based curve, calculated through linear regressions applied on the 10th to 30th minute interval.

Pathological grading of gliomas

Glioma classification according to the WHO 2016 standard was obtained from tumor samples provided by surgery or stereotactic biopsy [19]. IDH mutation status was assessed by immunohistochemistry with IDH1 R132H protein expression (Dianova, clone H09), or Sanger sequencing in case of ATRX immunohistochemical loss without IDH1 R132H staining [31]. Tumors presenting oligodendroglial morphology or showing IDH mutation without ATRX loss were additionally tested for 1p/19q co-deletion using multiplex PCR fragment analysis (loss of heterozygosity), or comparative genomic hybridization [26].

Statistical analysis

Categorical variables are expressed as percentages and continuous variables as medians (first quartile, third quartile). Intergroup comparisons were performed with Chi-squared tests for categorical variables and Mann-Whitney tests or Kruskal-Wallis tests for continuous variables. In the first step, Mann-Whitney tests were performed between gliomas with and without IDH mutation and additionally between gliomas with and without a 1p/19q co-deletion. A multivariate model including both static and dynamic parameters was applied for parameters reaching a sufficiently high level of significance at univariate analysis (probability value equal or less than 0.1). In the second step, Kruskal-Wallis tests were performed between the three following glioma groups: IDH mutant without 1p/19q co-deleted gliomas, IDH mutant with 1p/19q co-deleted gliomas, and IDH wildtype gliomas. Probability values of less than 0.05 were considered significant.

Receiver-operating-characteristic (ROC) curves were also tested for the prediction of molecular parameters (i.e., IDH mutation and 1p/19q co-deletion) by static and dynamic PET parameters. Optimal threshold values, extracted from the ROC curves, were considered to be those associated with the maximal value of the product of sensitivity by specificity. Analyses were performed with the SPSS (SPSS Statistics for Windows, Version 20.0. Armonk, NY: IBM Corp) software package.

Results

Patients

Fifty-eight patients (44.8 (34.2, 59.4) years old, 20 women) were retrospectively selected with histological diagnosis obtained by surgery ($n = 34$) or biopsy ($n = 24$): 21 IDH mutant without 1p/19 co-deletion (IDH+/1p19q−) gliomas, 16 IDH mutant with 1p/19q co-deletion (IDH+/1p19q+) gliomas, and 21 with IDH wildtype (IDH−) gliomas, according to the WHO 2016 classification (Table 1). Contrast enhancement on T1-weighted gadolinium-injected MRI was observed in 7 (33.3%) patients with IDH+/1p19q− gliomas, 2 (12.5%) patients with IDH+/1p19q+ gliomas, and 10 (47.6%) patients with IDH− gliomas (Table 1). The 10 tumors that could not be detected with ^{18}F-FDopa PET ($TBR_{max} < 1.6$) were only diffuse gliomas involving 5 IDH+/1p19q− gliomas (23.8% of this population), 2 IDH+/1p19q + gliomas (12.5% of this population) and 3 IDH− gliomas (14.3% of this population) (Table 1). No significant difference in Carbidopa premedication ($p = 0.27$) was noted among the 3 glioma groups (i.e., (i) IDH+/1p19q−, (ii) IDH+/1p19q+, and (iii) IDH− groups). All static and dynamic PET parameters did not significantly differ between anaplastic (grade III WHO 2016) and non-anaplastic gliomas (grade II WHO 2016) ($p > 0.54$).

Prediction of the IDH mutation and 1p/19q co-deletion statuses

Results of univariate analyses are depicted in Table 2 and ROC curves in Figs. 1 and 2. As detailed in Table 2, only dynamic parameters (i.e., TTP and slope) were significant univariate PET predictors of the IDH mutation status (for

Table 1 Patient characteristics

	Patients				Age (years), median (Q1, Q3)	Female gender, *n* (%)
	All (*n* = 58), *n* (%)	TBR_{max} < 1.6 (*n* = 10), *n* (%)	CE on MRI (*n* = 19), *n* (%)			
IDH+/1p19q− astrocytomas	12 (20.7%)	3 (30.0%)	4 (21.1%)	IDH+/1p19q− gliomas (*n* = 21)	37.3 (30.2, 49.9)	7 (33.3%)
Anaplastic IDH+/1p19q− astrocytomas	8 (13.8%)	2 (20.0%)	2 (10.5%)			
IDH+/1p19q− glioblastomas	1 (1.7%)	0 (0.0%)	1 (5.3%)			
IDH+/1p19q+ oligodendrogliomas	7 (12.1%)	0 (0.0%)	1 (5.3%)	IDH+/1p19q+ gliomas (*n* = 16)	38.8 (34.9, 58.2)	5 (31.3%)
Anaplastic IDH+/1p19q+ oligodendrogliomas	9 (15.5%)	2 (20.0%)	1 (5.3%)			
IDH− astrocytomas	6 (10.3%)	1 (10.0%)	0 (0.0%)	IDH− gliomas (*n* = 21)	58.6 (40.8, 69.5)†	8 (38.1%)
Anaplastic IDH− astrocytomas	5 (8.6%)	2 (20.0%)	1 (5.3%)			
IDH− glioblastomas	10 (17.2%)	0 (0.0%)	9 (47.4%)			
				p value	0.016*	0.901

*$p < 0.05$ for the global 3 groups comparisons

†$p < 0.05$ for comparison between IDH mutant and IDH wildtype gliomas

CE, contrast enhancement; *IDH+/1p19q−*, IDH mutant without 1p/19q co-deletion gliomas; *IDH+/1p19+*, IDH mutant with 1p/19q co-deletion gliomas; *IDH−*, IDH wildtype gliomas; *TBR*, tumor-to-brain ratio

TTP $p < 0.001$, area under the curve (AUC) = 0.789, and for slope $p = 0.013$ and AUC = 0.698) whereas TTP was the sole significant predictor of the 1p/19q co-deletion status ($p = 0.034$ and AUC = 0.679). The global accuracies for predicting the IDH mutation status reached 74% (sensitivity 76%, specificity 73%) when using the criterion of a TTP ≥ 5.4 min, and 62% (sensitivity 67%, specificity 59%) when using the criterion of a slope ≥ − 0.39 h^{-1} (Fig. 1). For the prediction of the 1p/19q co-deletion status, a global diagnostic accuracy of 69% (sensitivity 69%, specificity 69%) was achieved when using the criterion of a TTP ≥ 6.9 min (Fig. 2). No static parameter reached a sufficiently high level of significance at univariate analysis (Table 2) to be tested in a multivariate model together with the significant univariate dynamic parameters (Fig. 3).

Prediction of IDH+/1p19q− gliomas, IDH+/1p19q+ gliomas, and IDH− gliomas

Intergroup comparisons of PET parameters in each of the three glioma groups are given in Table 3. TTP was the only

Table 2 Results of the univariate analyses for predicting IDH mutation and 1p/19q co-deletion statuses with the considered static and dynamic PET variables

Parameter	*p* value	AUC	Cut-off	Sensitivity	Specificity	Accuracy
IDH mutation status						
TSR_{mean}	0.704	NS	–	–	–	–
TSR_{max}	0.955	NS	–	–	–	–
TBR_{mean}	0.523	NS	–	–	–	–
TBR_{max}	0.734	NS	–	–	–	–
MTV (mL)	0.740	NS	–	–	–	–
TTP (min)	< 0.001*	0.789	≥ 5.4	76%	73%	74%
Slope (h^{-1})	0.013*	0.698	≥ − 0.39	67%	59%	62%
1p/19q co-deletion status						
TSR_{mean}	0.708	NS	–	–	–	–
TSR_{max}	0.429	NS	–	–	–	–
TBR_{mean}	0.931	NS	–	–	–	–
TBR_{max}	0.774	NS	–	–	–	–
MTV (mL)	0.531	NS	–	–	–	–
TTP (min)	0.034*	0.679	≥ 6.9	69%	69%	69%
Slope (h^{-1})	0.186	NS	–	–	–	–

*p value < 0.05; *AUC*, area under the curve; *MTV*, metabolic tumor volume; *NS*, non-significant; *TBR*, tumor-to-brain ratio; *TSR*, tumor-to-striatum ratio; *TTP*, time-to-peak

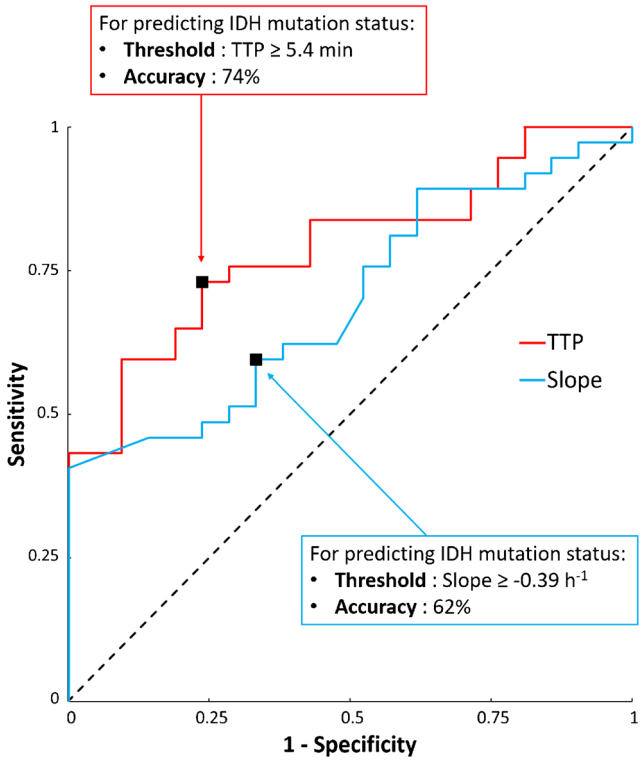

Fig. 1 ROC curves illustrating the sensitivity and specificity of TTP and slope in predicting IDH mutation status. Optimal thresholds and its associated accuracies are indicated

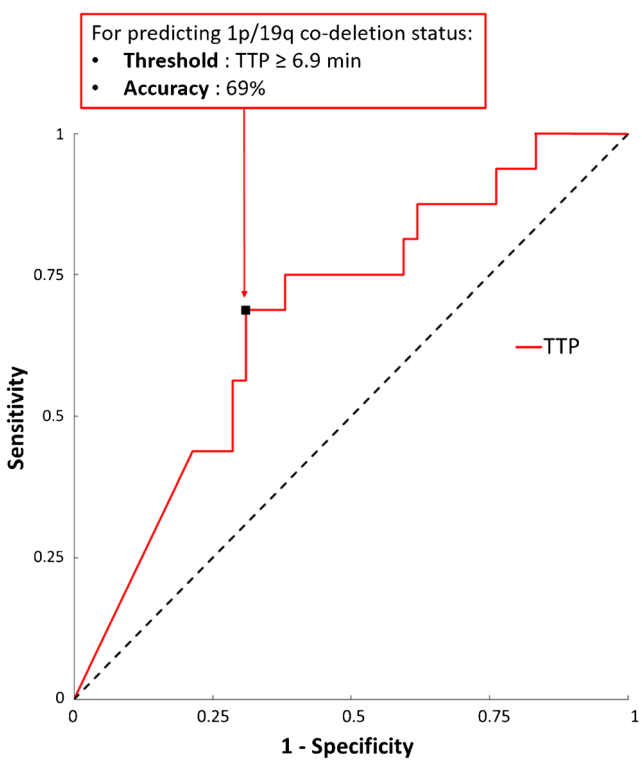

Fig. 2 ROC curves illustrating the sensitivity and specificity of TTP in predicting 1p/19q co-deletion status. Optimal threshold and its associated accuracy are indicated

significant univariate PET predictor of this 3-group comparison discriminating IDH− gliomas from IDH+/1p19q− gliomas ($p = 0.007$, AUC = 0.766, cut-off 5.1 min, accuracy 74%, sensitivity 76%, specificity 71%) as well as IDH+/1p19q+ gliomas ($p = 0.003$, AUC = 0.818, cut-off 6.2 min, accuracy 78%, sensitivity 75%, specificity 81%).

Discussion

The present study shows that the prediction of the molecular features according to the WHO 2016 classification of newly diagnosed gliomas with ^{18}F-FDopa PET imaging and especially the assessment of IDH mutation is achieved owing exclusively to dynamic parameters, and especially TTP. Dynamic ^{18}F-FDopa PET parameters were able to discriminate IDH wildtype gliomas from the IDH mutant gliomas associated or not with a 1p/19q co-deletion, underlying the more general information that IDH mutation can be predicted non-invasively to a certain level by ^{18}F-FDopa PET. The dynamic PET TTP parameter was additionally found to be a predictor of the 1p/19q co-deletion status, although at a lower level of significance.

To date, the characterization of gliomas with dynamic analyses of ^{18}F-FDopa PET has been reported in only a few studies, which were furthermore performed with compartmental models and involved limited numbers of patients (16 to 37), all of which had inconclusive or poorly conclusive results [16–18]. These previous studies were moreover based on the 2007 WHO classification of gliomas [32], whereas the WHO 2016 classification, including molecular parameters, provides a much more accurate characterization with regard to prognostic and therapeutic outcomes [19]. This recent upgrade in the WHO classification is mainly related to the introduction of molecular parameters of high prognostic and therapeutic significance, especially the presence or absence of IDH mutation and 1p/19q co-deletion [19]. In addition, the use of dynamic analysis with ^{18}F-FDopa PET is not yet proposed in the recent EANM guidelines for brain tumor imaging [28].

The present study proposes a simple approach for the dynamic analysis of ^{18}F-FDopa PET, easily transposable to clinical practice and comparable with that previously validated in a similar setting for ^{18}F-FET, another amino acid PET radiotracer [14, 15].

As a result, the use of the dynamic TTP parameter enabled a non-invasive prediction of the IDH mutation status independently of the presence or absence of an additional 1p/19q co-deletion. The IDH wildtype gliomas exhibited a particularly short TTP, a feature currently considered to characterize those gliomas associated with a particularly poor outcome [33]. From a clinical standpoint, differentiating the group of IDH wildtype gliomas from IDH mutant gliomas with a non-invasive method is particularly useful, thereby favoring the

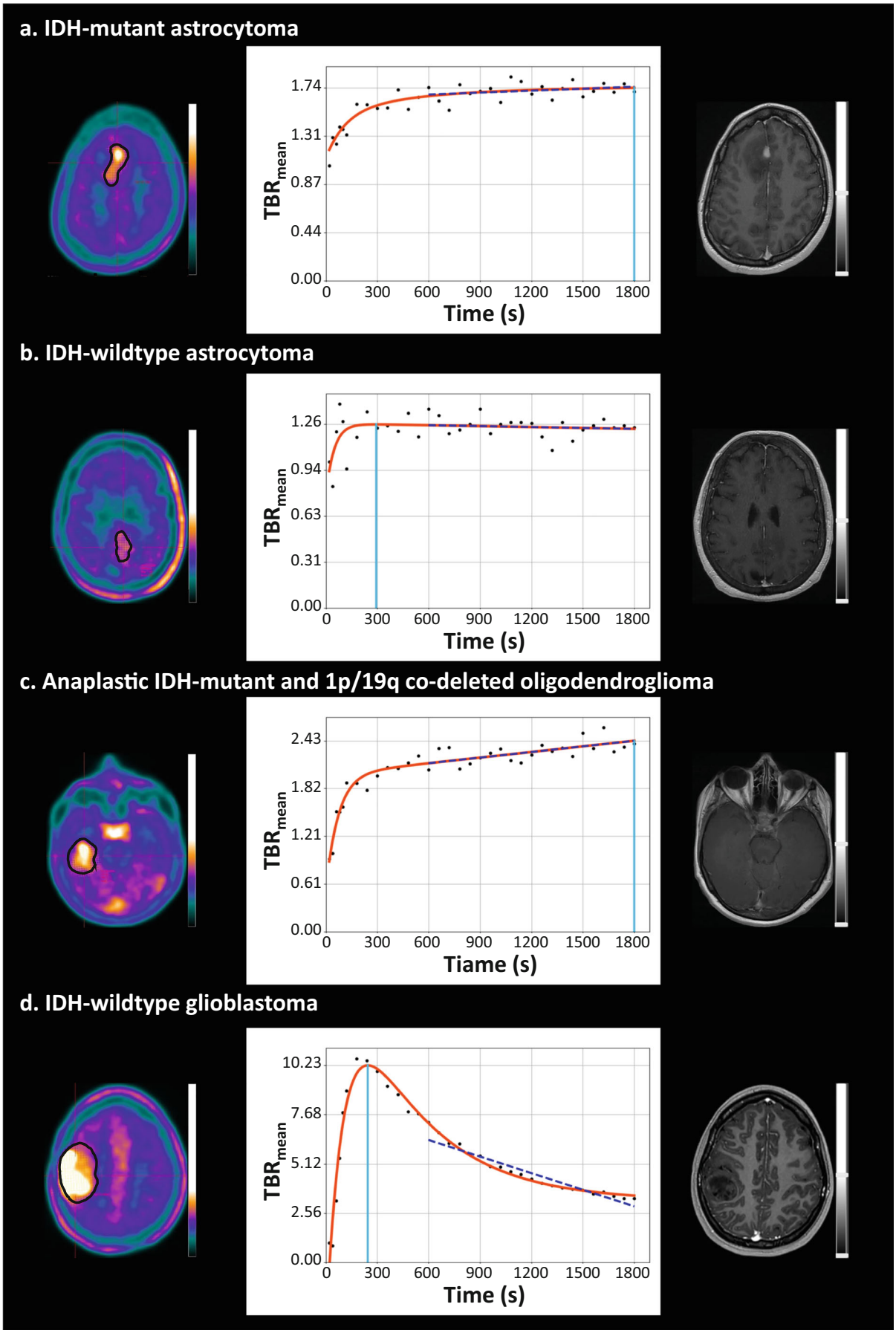

Table 3 Median (interquartile range) of all considered static or dynamic PET parameters in each of the three glioma groups with the results of intergroup comparisons

Parameter	IDH+/1p19q− ($n = 21$)	IDH+/1p19q+ ($n = 16$)	IDH− ($n = 21$)	p value
TSR_{mean}	1.04 (0.88, 1.29)	1.30 (0.95, 1.55)	1.16 (0.88, 1.49)	0.687
TSR_{max}	1.91 (1.30,2.42)	2.16 (1.45, 3.06)	2.38 (1.33, 3.32)	0.766
TBR_{mean}	1.35 (1.24, 1.73)	1.58 (1.24, 2.01)	1.63 (1.23, 2.23)	0.832
TBR_{max}	2.54 (1.66, 3.39)	2.94 (1.88, 4.08)	3.33 (1.73, 4.81)	0.742
MTV (mL)	16.60 (2.34, 37.24)	25.97 (12.98, 42.40)	17.88 (2.58; 62.23)	0.642
TTP (min)	7.87 (4.81;30.00)†	10.85 (5.09, 30)†	4.09 (2.64, 5.69)	0.001*
Slope (h^{-1})	− 0.12 (− 0.85, 0.13)	− 0.29 (− 1.27, 0.29)	− 0.65 (− 2.20, −0.14)	0.05

*$p < 0.05$ for intergroup comparison between 3 groups

†$p < 0.05$ for comparison with IDH− gliomas

IDH+/1p19q−, IDH mutant without 1p/19q co-deletion gliomas; *IDH+/1p19+*, IDH mutant with 1p/19q co-deletion gliomas; *IDH−*, IDH wildtype gliomas; *MTV*, metabolic tumor volume; *TBR*, tumor-to-brain ratio; *TSR*, tumor-to-striatum ratio; *TTP*, time-to-peak

identification of patients for whom initiating treatment cannot be delayed [34]. It is even more important when dealing with IDH wildtype diffuse gliomas where searching for MRI contrast enhancement is unfortunately weakly contributive (only one patient with IDH wildtype astrocytoma exhibited contrast enhancement on MRI in the present study (see Table 1)). On the other hand, predicting the IDH mutant gliomas conferring a better prognosis [33] could benefit elderly patients presenting high rates of clinical deficit at initial diagnosis and for whom biopsy or surgery is particularly at risk [35].

Moreover, our results suggest that TTP may also provide a certain degree of prediction of the 1p/19q co-deletion status. This prediction may be obtained with the criterion of a particularly long TTP, of at least 6.9 min, in contrast to the most aggressive IDH wildtype entities. This additional observation is also of particular importance since gliomas with both IDH mutation and a 1p/19q co-deletion are currently characterized by high amino acid uptakes, notably with ^{18}F-FET and ^{11}C-methionine PET, which may lead to a difficult differentiation from glioblastoma in static analyses [36–38].

In addition, one PET study performed with another amino acid, ^{11}C-methionine, had proposed to discriminate the oligodendroglial component of gliomas through the criterion of a lower slope at the late phase [39]. These results are clearly different from those of the present ^{18}F-FDopa study, confirming that the kinetics information provided by the different amino acid radiotracers is not comparable in this clinical setting [40].

The mechanisms leading to the tumor uptake of amino acid radiotracers have mostly been analyzed for ^{18}F-FET and still remain to be fully understood, particularly for ^{18}F-FDopa. While it is generally considered that the uptake of ^{18}F-FDopa is carried out with the L-system amino acid transporters and in particular, with the LAT1 transporters which are over-expressed in gliomas, the intensity of ^{18}F-FDopa uptake is nonetheless not correlated with the level of LAT1 expression [41]. Indeed, the tumor uptake of amino acid tracers is also correlated with cell proliferation and microvessel density, with a disruption of the blood brain barrier likely facilitating the initial tumor uptake of the tracers, as well as their subsequent passive back diffusion [42]. It must nevertheless be pointed out that the faster kinetics observed herein for certain tumors is not solely explained by the breakdown of the blood brain barrier. This is particularly the case for our eleven IDH wildtype astrocytomas for which the kinetics were in most of cases particularly fast, with short TTP and negative slope, whereas the MRI contrast enhancement, which accompanies the breakdown of the blood brain barrier, was observed in only one of these IDH wildtype astrocytomas (Table 1).

In high-grade tumors, the breakdown of the blood brain barrier, but also microvessel density and LAT1 expression, are particularly manifest [42], thereby explaining our observations of a faster uptake and a faster washout of ^{18}F-FDopa within the IDH wildtype gliomas. This consideration is

◀ **Fig. 3** Representative examples of metabolic tumor volume delineation for each glioma group, performed on an axial slice of ^{18}F-FDopa PET (left column) with the dynamic TBR_{mean} curve (middle column) providing the time-to-peak delay-time (light blue line) and the 10 to 30 min slope (dark blue line), along with, for illustration purposes, the same slice location recorded on contrast-enhanced T1-weighted MRI (right column). **a** 27-year-old woman with an IDH mutant astrocytoma with contrast enhancement on T1-weighted gadolinium-injected MRI (TBR_{mean} of 1.4, TBR_{max} of 2.7, TSR_{mean} of 1, TSR_{max} of 2, MTV of 16.6 ml, TTP of 30 min, and slope of 0.21 h^{-1}). **b** 79-year-old woman with an IDH wildtype astrocytoma without contrast enhancement on T1-weighted gadolinium-injected MRI (TBR_{mean} of 1.3, TBR_{max} of 1.6, TSR_{mean} of 1, TSR_{max} of 1.2, MTV of 12.3 mL, TTP of 4.9 min, and slope of − 0.07 h^{-1}). **c** 57-year-old woman with an anaplastic IDH mutant and 1p/19q co-deleted oligodendroglioma without contrast enhancement on T1-weighted gadolinium-injected MRI (TBR_{mean} of 1.7, TBR_{max} of 2.8, TSRmean of 1.3, TSR_{max} of 2.2, MTV of 27.5 mL, TTP of 30 min, and slope of 0.86 h^{-1}). **d** 22-year-old woman with an IDH wildtype glioblastoma with contrast enhancement on T1-weighted gadolinium-injected MRI (TBR_{mean} of 2.7, TBR_{max} of 5.3, TSR_{mean} of 2.2, TSR_{max} of 4.2, MTV of 73 ml, TTP of 4.1 min, and slope of − 10.34 h^{-1})

supported by previous kinetic modeling studies where high-grade tumors, representing the most aggressive entities, were found exhibiting the highest transport rate constant [16].

Up to now, no previous ^{18}F-FDopa PET imaging study had been conducted to discriminate the molecular features of gliomas according to the WHO 2016 classification in a population including both diffuse gliomas and glioblastomas and using dynamic parameters. A few studies [24–26] had already attempted to characterize these molecular features with static parameters and in populations including (i) both diffuse gliomas and glioblastomas but with inconclusive results with regard to the discrimination of IDH mutation or 1p/19q co-deletion [24] and (ii) only diffuse gliomas and with results showing a significantly higher ^{18}F-FDopa uptake in IDH mutant gliomas comparatively with the IDH wildtype gliomas [25, 26]. These findings are in accordance with those from the present study in which no static parameter was able to discriminate the molecular features of gliomas in our admixed population of diffuse gliomas and glioblastomas. In addition, we also found that the IDH wildtype diffuse gliomas (IDH wildtype astrocytomas) showed a significantly lower MTV than IDH mutant diffuse gliomas (IDH mutant astrocytomas and IDH mutant and 1p/19q co-deleted oligodendrogliomas) (see additional results in Supplemental Fig. 2). It should also be pointed out that glioblastomas (grade IV gliomas) were able to be discriminated herein from all other gliomas with the dual criterion of a high MTV and short TTP ($p < 0.01$, accuracy of 95%, see Supplemental Fig. 2).

Our retrospectively selected study population represents a particular and highly selected group, even if the proportions of the different glioma types fit well with data from epidemiological studies [43]. Nevertheless, extrapolation to more general populations should be carried out with caution, particularly for the diagnostic thresholds and performances documented herein for the prediction of each glioma type with ^{18}F-FDopa PET. It should additionally be pointed out that the TAC ratios used in the present study likely allow overcoming a possible interference of Carbidopa premedication taken by certain patients [27], thereby rendering our results as independent as possible of this premedication. Notwithstanding, close results were documented when SUV values were used instead of TBR for TAC in the present study, with dynamic parameters being the sole predictors, namely (1) TTP and slope for IDH mutation and (2) slope for 1p/19q co-deletion (results not shown). Finally, it should also be kept in mind that dynamic analyses could only be obtained with a dual analysis of MRI images in instances of a very low tumor uptake of ^{18}F-FDopa PET. This was the case of 17% of our patients, a proportion comparable with those previously documented in other amino acid PET studies [44, 45].

Altogether, the present study highlights the significant added value of including dynamic parameters for the routine analysis of the ^{18}F-FDopa PET imaging of gliomas. The latter is indeed associated with a marked improvement in the characterization of molecular features of newly diagnosed gliomas according to the WHO 2016 classification, especially for the non-invasive identification of IDH mutation status. These findings need to be further confirmed in larger scale prospective trials involving additional clinical and MRI variables of interest, in order to improve the non-invasive prediction of glioma types as well as to optimize patient management. Further clinical questions involving ^{18}F-FDopa PET imaging in gliomas such as recurrence or treatment monitoring could also be assessed by integrating these dynamic parameters.

Acknowledgments The authors thank Pierre Pothier for his critical review of the manuscript.

Compliance with ethical standards

Conflict of interest The authors declare that they have no conflict of interest.

Ethical approval All procedures performed in studies involving human participants were in accordance with the ethical standards of the institutional and/or national research committee and with the 1964 Helsinki declaration and its later amendments or comparable ethical standards.

Informed consent Informed written consent was obtained from all individual participants included in the study.

References

1. Langen K-J, Galldiks N, Hattingen E, Shah NJ. Advances in neuro-oncology imaging. Nat Rev Neurol. 2017;13:279.
2. Langen K-J, Galldiks N. Update on amino acid PET of brain tumours. Curr Opin Neurol. 2018;31:354–61.
3. Galldiks N, Langen K-J. Amino acid PET in neuro-oncology: applications in the clinic. Expert Rev Anticancer Ther. 2017;17:395–7.
4. Verger A, Langen KJ. PET Imaging in Glioblastoma: use in clinical practice. In: De Vleeschouwer S, editor. Glioblastoma. Brisbane (AU): Codon Publications; 2017. pp. 155–174.
5. Verger A, Arbizu J, Law I. Role of amino-acid PET in high-grade gliomas: limitations and perspectives. Q J Nucl Med Mol Imaging. 2018;62:254–66.
6. Albert NL, Weller M, Suchorska B, Galldiks N, Soffietti R, Kim MM, et al. Response assessment in neuro-oncology working group and European Association for Neuro-Oncology recommendations for the clinical use of PET imaging in gliomas. Neuro-Oncol. 2016;18:1199–208.
7. Chen W, Silverman DHS, Delaloye S, Czernin J, Kamdar N, Pope W, et al. 18F-FDOPA PET imaging of brain tumors: comparison study with 18F-FDG PET and evaluation of diagnostic accuracy. J Nucl Med. 2006;47:904–11.
8. Fueger BJ, Czernin J, Cloughesy T, Silverman DH, Geist CL, Walter MA, et al. Correlation of 6-18F-Fluoro-L-Dopa PET uptake with proliferation and tumor grade in newly diagnosed and recurrent gliomas. J Nucl Med. 2010;51:1532–8.
9. Janvier L, Olivier P, Blonski M, Morel O, Vignaud J-M, Karcher G, et al. Correlation of SUV-derived indices with tumoral

aggressiveness of gliomas in static 18F-FDOPA PET: use in clinical practice. Clin Nucl Med. 2015;40:e429–35.
10. Humbert O, Bourg V, Mondot L, Gal J, Bondiau P-Y, Fontaine D, et al. 18F-DOPA PET/CT in brain tumors: impact on multidisciplinary brain tumor board decisions. Eur J Nucl Med Mol Imaging. 2019;46:558–68.
11. Bund C, Heimburger C, Imperiale A, Lhermitte B, Chenard M-P, Lefebvre F, et al. FDOPA PET-CT of nonenhancing brain tumors. Clin Nucl Med. 2017;42:250–7.
12. Patel CB, Fazzari E, Chakhoyan A, Yao J, Raymond C, Nguyen H, et al. 18F-FDOPA PET and MRI characteristics correlate with degree of malignancy and predict survival in treatment-naïve gliomas: a cross-sectional study. J Neuro-Oncol. 2018;139:399–409.
13. Schwarzenberg J, Czernin J, Cloughesy TF, Ellingson BM, Pope WB, Grogan T, et al. Treatment response evaluation using 18F-FDOPA PET in patients with recurrent malignant glioma on bevacizumab therapy. Clin Cancer Res. 2014;20:3550–9.
14. Pöpperl G, Kreth FW, Mehrkens JH, Herms J, Seelos K, Koch W, et al. FET PET for the evaluation of untreated gliomas: correlation of FET uptake and uptake kinetics with tumour grading. Eur J Nucl Med Mol Imaging. 2007;34:1933–42.
15. Lohmann P, Herzog H, Rota Kops E, Stoffels G, Judov N, Filss C, et al. Dual-time-point O-(2-[18F]fluoroethyl)-L-tyrosine PET for grading of cerebral gliomas. Eur Radiol. 2015;25:3017–24.
16. Schiepers C, Chen W, Cloughesy T, Dahlbom M, Huang S-C. 18F-FDOPA kinetics in brain tumors. J Nucl Med. 2007;48:1651–61.
17. Nioche C, Soret M, Gontier E, Lahutte M, Dutertre G, Dulou R, et al. Evaluation of quantitative criteria for glioma grading with static and dynamic 18F-FDopa PET/CT. Clin Nucl Med. 2013;38:81–7.
18. Kratochwil C, Combs SE, Leotta K, Afshar-Oromieh A, Rieken S, Debus J, et al. Intra-individual comparison of 18F-FET and 18F-DOPA in PET imaging of recurrent brain tumors. Neuro-Oncol. 2014;16:434–40.
19. Louis DN, Perry A, Reifenberger G, von Deimling A, Figarella-Branger D, Cavenee WK, et al. The 2016 World Health Organization classification of tumors of the central nervous system: a summary. Acta Neuropathol (Berl). 2016;131:803–20.
20. Lopci E, Riva M, Olivari L, Raneri F, Soffietti R, Piccardo A, et al. Prognostic value of molecular and imaging biomarkers in patients with supratentorial glioma. Eur J Nucl Med Mol Imaging. 2017;44:1155–64.
21. Verger A, Stoffels G, Bauer EK, Lohmann P, Blau T, Fink GR, et al. Static and dynamic 18F–FET PET for the characterization of gliomas defined by IDH and 1p/19q status. Eur J Nucl Med Mol Imaging. 2018;45:443–51.
22. Kebir S, Weber M, Lazaridis L, Deuschl C, Schmidt T, Mönninghoff C, et al. Hybrid 11C-MET PET/MRI combined with "Machine Learning" in glioma diagnosis according to the revised glioma WHO classification 2016. Clin Nucl Med. 2019;44:214–20.
23. Suchorska B, Giese A, Biczok A, Unterrainer M, Weller M, Drexler M, et al. Identification of time-to-peak on dynamic 18F-FET-PET as a prognostic marker specifically in IDH1/2 mutant diffuse astrocytoma. Neuro-Oncol. 2018;20:279–88.
24. Cicone F, Carideo L, Scaringi C, Arcella A, Giangaspero F, Scopinaro F, et al. 18F-DOPA uptake does not correlate with IDH mutation status and 1p/19q co-deletion in glioma. Ann Nucl Med. 2019;33:295–302.
25. Verger A, Metellus P, Sala Q, Colin C, Bialecki E, Taieb D, et al. IDH mutation is paradoxically associated with higher 18F-FDOPA PET uptake in diffuse grade II and grade III gliomas. Eur J Nucl Med Mol Imaging. 2017;44:1306–11.
26. Isal S, Gauchotte G, Rech F, Blonski M, Planel S, Chawki MB, et al. A high 18F-FDOPA uptake is associated with a slow growth rate in diffuse Grade II–III gliomas. Br J Radiol. 2018;91(1084):20170803.
27. Hoffman JM, Melega WP, Hawk TC, Grafton SC, Luxen A, Mahoney DK, et al. The effects of carbidopa administration on 6-[18F]fluoro-L-dopa kinetics in positron emission tomography. J Nucl Med. 1992;33:1472–7.
28. Law I, Albert NL, Arbizu J, Boellaard R, Drzezga A, Galldiks N, et al. Joint EANM/EANO/RANO practice guidelines/SNMMI procedure standards for imaging of gliomas using PET with radiolabelled amino acids and [18F]FDG: version 1.0. Eur J Nucl Med Mol Imaging. 2019;46:540–57.
29. Ye H, Wong K-P, Wardak M, Dahlbom M, Kepe V, Barrio JR, et al. Automated movement correction for dynamic PET/CT images: evaluation with phantom and patient data. Chen K, editor. PLoS ONE. 2014;9:e103745.
30. Ceccon G, Lohmann P, Stoffels G, Judov N, Filss CP, Rapp M, et al. Dynamic O-(2-18F-fluoroethyl)-L-tyrosine positron emission tomography differentiates brain metastasis recurrence from radiation injury after radiotherapy. Neuro-Oncol. 2017;19:281–8.
31. Perizzolo M, Winkfein B, Hui S, Krulicki W, Chan JA, Demetrick DJ. IDH mutation detection in formalin-fixed paraffin-embedded gliomas using multiplex PCR and single-base extension: IDH1/2 mutation detection by SNaPshot®. Brain Pathol. 2012;22:619–24.
32. Louis DN, Ohgaki H, Wiestler OD, Cavenee WK, Burger PC, Jouvet A, et al. The 2007 WHO classification of tumours of the central nervous system. Acta Neuropathol (Berl). 2007;114:97–109.
33. The Cancer Genome Atlas Research Network. Comprehensive, integrative genomic analysis of diffuse lower-grade gliomas. N Engl J Med. 2015;372:2481–98.
34. Pallud J, Blonski M, Mandonnet E, Audureau E, Fontaine D, Sanai N, et al. Velocity of tumor spontaneous expansion predicts long-term outcomes for diffuse low-grade gliomas. Neuro-Oncol. 2013;15:595–606.
35. Kaloshi G, Psimaras D, Mokhtari K, Dehais C, Houillier C, Marie Y, et al. Supratentorial low-grade gliomas in older patients. Neurology. 2009;73:2093–8.
36. Jansen NL, Schwartz C, Graute V, Eigenbrod S, Lutz J, Egensperger R, et al. Prediction of oligodendroglial histology and LOH 1p/19q using dynamic [18F]FET-PET imaging in intracranial WHO grade II and III gliomas. Neuro-Oncol. 2012;14:1473–80.
37. Manabe O, Hattori N, Yamaguchi S, Hirata K, Kobayashi K, Terasaka S, et al. Oligodendroglial component complicates the prediction of tumour grading with metabolic imaging. Eur J Nucl Med Mol Imaging. 2015;42:896–904.
38. Bashir A, Brennum J, Broholm H, Law I. The diagnostic accuracy of detecting malignant transformation of low-grade glioma using O-(2-[18F]fluoroethyl)-l-tyrosine positron emission tomography: a retrospective study. J Neurosurg. 2018;130:451–64.
39. Nomura Y, Asano Y, Shinoda J, Yano H, Ikegame Y, Kawasaki T, et al. Characteristics of time-activity curves obtained from dynamic 11C-methionine PET in common primary brain tumors. J Neuro-Oncol. 2018;138:649–58.
40. Verger A, Taieb D, Guedj E. Is the information provided by amino acid PET radiopharmaceuticals clinically equivalent in gliomas? Eur J Nucl Med Mol Imaging. 2017;44:1408–10.
41. Dadone-Montaudié B, Ambrosetti D, Dufour M, Darcourt J, Almairac F, Coyne J, et al. [18F] FDOPA standardized uptake values of brain tumors are not exclusively dependent on LAT1 expression. PLoS One. 2017;12:e0184625.
42. Pöpperl G, Kreth FW, Herms J, Koch W, Mehrkens JH, Gildehaus FJ, et al. Analysis of 18F-FET PET for grading of recurrent gliomas: is evaluation of uptake kinetics superior to standard methods? J Nucl Med. 2006;47:393–403.
43. Jiang H, Cui Y, Wang J, Lin S. Impact of epidemiological characteristics of supratentorial gliomas in adults brought about by the 2016 world health organization classification of tumors of the central nervous system. Oncotarget. 2017;8:20354–61.

44. Jansen NL, Suchorska B, Wenter V, Schmid-Tannwald C, Todica A, Eigenbrod S, et al. Prognostic significance of dynamic 18F-FET PET in newly diagnosed astrocytic high-grade glioma. J Nucl Med. 2015;56:9–15.
45. Unterrainer M, Schweisthal F, Suchorska B, Wenter V, Schmid-Tannwald C, Fendler WP, et al. Serial 18F-FET PET imaging of primarily 18F-FET-negative glioma: does it make sense? J Nucl Med. 2016;57:1177–82.